18th Australasian Fluid Mechanics Conference
Launceston, Australia
3-7 December 2012

Aeroacoustic resonance in a rectangular cavity: Part 1 effect of Mach number and Reynolds number

M. B. Jones[1], S. M. Henbest[1], J. H. Watmuff[2] and A. Blandford[1]

[1]Air Vehicles Division, Defence Science and Technology Organisation, Melbourne, Victoria, 3207 Australia
[2] School of Aerospace, Mechanical and Manufacturing Engineering, RMIT University, Bundoora, Victoria, 3083 Australia

Abstract

An experimental study of flow over a generic cavity has been undertaken. Measurements of the fluctuating pressures within a cavity are presented. Cavity models having lengths of 200 and 250 mm and a depth of 50 mm were tested under freestream Mach numbers ranging between 0.3 to 1.3. Due to the coupling of the aerodynamic and acoustic fields, feedback loops can be established resulting in cavity resonance and on aircraft, these high-intensity acoustic tones may lead to noise radiation, structural fatigue, and interference with on-board avionic systems. The purpose of this experimental program is to understand the conditions leading to this resonance and the effect of a range of parameters on both the frequencies and intensities of the tones. In this paper we focus mostly on Mach number and Reynolds number dependency. There was found to be no observed dependency on the Reynolds number, across the Reynolds number range of 27×10^6 to 81×10^6 per metre. Both the (non-dimensional) frequencies and intensities varied with Mach number. The resonant frequencies observed were consistent with the semi-empirical feedback model of Rossiter [10]

Introduction

Predicting and understanding the aeroacoustic phenomena associated with cavity flows is important from a practical point of view. For example, cavity type geometries exist on the external surfaces of aircraft in the form of: landing-gear wells, weapon bays, fuel vent recesses and instrumentation recesses.

The acoustics of rectangular cavities have been studied by many workers both experimentally and computationally. Seminal work by [10] on rectangular cavities showed that the Strouhal number, St, depended on the resonance mode, m, the Mach number, M, as follows

$$St = \frac{fL}{U_\infty} = \frac{m-\gamma}{M+\frac{1}{K}} \qquad (1)$$

where γ and K are empirically determined constants, f is the resonance frequency, L is the cavity length and U_∞ the free stream velocity. Usually the constant are taken to be $K=0.57$ and $\gamma=0.25$, based largely on the original data of [10]. While (1) establishes what modes may exist, it does not provide any indication whether acoustic resonance will occur nor which mode is likely to be dominant.

The authors have carried out a literature review of the existing data, as well as empirically based and analytical based prediction methods [7]. Based on these reviews it was concluded that the conditions leading to cavity resonance are not well defined. Criteria for a resonant condition have been proposed by various authors for example see [4], [12], [2], [11]. However often such criteria are limited to a particular cavity geometry, Mach number or Reynolds number range.

The number of relevant parameters influencing cavity resonance may be large and includes: cavity geometry, upstream influence, Mach number, Reynolds number, boundary layer thickness and state (laminar or turbulent). Attempts have been made in the past to incorporate such parameters into (1). For example modifications to Rossiter's model of are given by [2], who included the effect of cavity length to depth, and [13], who included effects of upstream boundary layer momentum thickness. There is little published flight-test data (full scale data); hence, the accuracy of scaling wind tunnel data to flight conditions remains unclear.

The purpose of this work is to undertake systematic experiments across a range of Mach numbers, cavity geometries and length scales (e.g. upstream boundary layer thickness relative to cavity scale). To date the authors have experimentally investigated the effects of Mach number, Reynolds number, cavity yaw angle and cavity geometry (length-to-depth and variations to leading and trailing edges). In this paper the effects of Mach number, Reynolds number and length-to-depth ratio are presented. A companion paper [6] presents the effect of yaw angle and cavity leading and trailing edge geometries.

Experimental method

Transonic wind tunnel

The DSTO transonic wind tunnel (TWT) is a closed return-circuit continuous flow tunnel with a Mach number range from $M=0.30$ to approximately 1.30 continuously variable (the upper limit depend on model blockage). The tunnel total pressure can be varied from 30 kPa to 200 kPa via a plenum evacuation system and this allows for independent control of the Mach number and Reynolds number (Re). The variation of Re with M for a fixed total pressure, p_0, is given in figure 1 and the (M,Re) experimental test matrix is marked on this chart.

The test section is 0.8 m wide by 0.8 m high with slotted top and bottom walls. Solid sidewalls were installed for this test entry. A turntable in the inner sidewall provides a yaw capability of $\pm90°$.

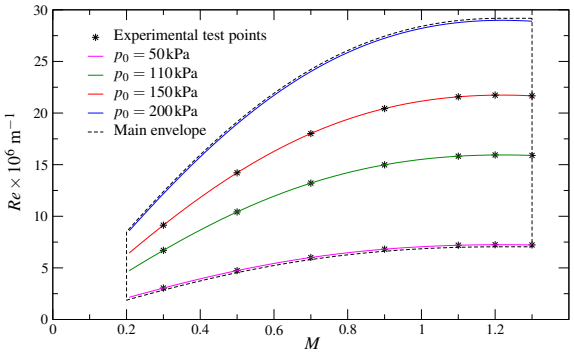

Figure 1: Variation of Re with M for fixed values of p_0. Dashed line gives the main operational envelope of the tunnel with an empty test section.

Cavity model and instrumentation

A cavity plug insert was manufactured so that it could be installed via the sidewall turntable, figure 2. The regular cavity had a length of $L = 250\,\text{mm}$, a depth of $D = 50\,\text{mm}$ and a width of $W = 50\,\text{mm}$. A series of insert blocks where manufactured to fit at the leading and trailing edge of the regular cavity. The purpose of the blocks was to study the effect of yawed and inclined leading and trailing edges. The inserts were designed to maintain an $L/D = 4$, where L is measured along the open face centre-line.

The fluctuating pressures were measured using *Kulite Semiconductor* model XT-140m-25A pressure transducers which are rated to 25 PSI and measure absolute pressure. The transducers have a linear response with a nominal full scale output of 100 mV. The natural frequency of the sensors is nominally 50 kHz and this far exceeds the frequencies of interest, which are less than 2.5 kHz. The Kulite pressure transducer is a strain gauge device which is amplified using a *Dewetron* strain gauge amplifier before being sampled by a 24-bit data acquisition board, which can sample 16 channels simultaneously. All signals were sampled for a period of $T = 40\,\text{seconds}$, at a sampling rate of 7 kHz. The strain gauge amplifier also provides filtering capabilities and the filters were set to low pass *Butterworth* type with a cut off frequency of 3 kHz. The Kulite locations and main reference dimensions of the cavity are shown in Figure 3.

Along with the Kulite signals, the tunnel stagnation pressure and temperature and the working section static pressure and temperature were measured simultaneously.

All measurements were performed with the plug centre positioned at a streamwise location 1652 mm from the start of the working section. The boundary layer profile, 25 mm upstream of the cavity leading edge, was determined by traversing a Pitot tube from the wall into the freestream. The static pressure was measured from a static tapping placed slightly upstream of the Pitot station. The Pitot and static pressures were measured with Digiquartz 23 PSI absolute transducers.

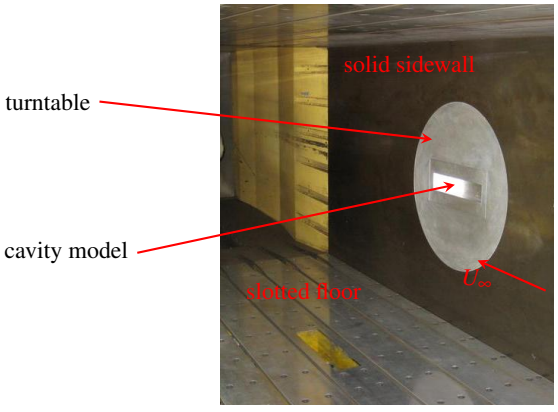

Figure 2: Cavity model installed in solid sidewall of working section.

Experimental Results

Upstream boundary layer

An experimental study by [1] found the thickness of the upstream turbulent boundary layer, relative to the cavity dimensions, influenced the intensity of the resonant tones. For their experiment, a change of $L/\delta = 26.6$ to $L/\delta = 15.1$ caused the tones to be entirely suppressed, where δ is the boundary layer thickness. For this reason the boundary layer profile 25 mm upstream of the cavity was measured using a Pitot tube referenced to a wall static pressure.

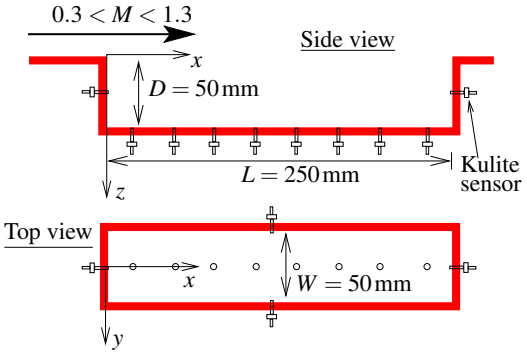

Figure 3: Side view of cavity showing location of Kulites on the cavity base, front and rear walls. Dimensions are shown for the $L/D = 5$ case. The $L/D = 4$ case has a reduced length of 200 mm.

The mean streamwise velocity profiles for the range of Mach numbers and the case of $p_0 = 50\,\text{kPa}$, are plotted in figure 4 and are consistent with a turbulent velocity profile. The velocity profiles in figure 4 are normalised with the friction velocity, U_τ, and this velocity was determined using a Clauser chart method [3]. Similar results were obtained for the other p_0 values.

The boundary layer thickness upstream of the cavity varied between approximately 17 mm to 27 mm across the range of the experiments and this corresponded to a L/δ range of 14 to 9 respectively. This variation was primarily due to Mach number and for a given p_0 the boundary layer thickness was found to reduce with increasing Mach number. While the value of p_0 also influenced δ, the effect was small and for fixed Mach number the maximum change in boundary layer thickness when p_0 was varied was around 3 mm. For this reason it was not possible to isolate the effect of boundary layer thickness on the intensity of the resonant tones.

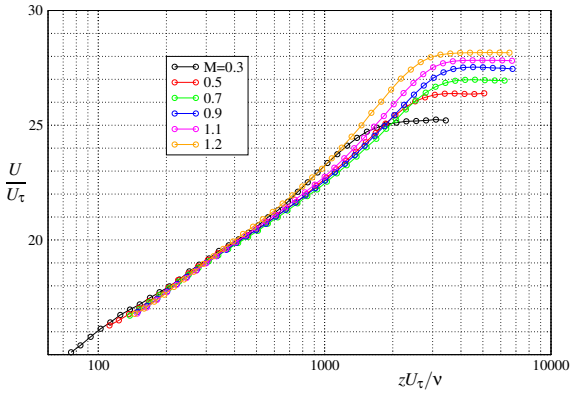

Figure 4: Mean streamwise velocity profile measured in the boundary layer for the range of Mach numbers and the case of $p_0 = 50\,\text{kPa}$, where U is the streamwise velocity, ν is the kinematic viscosity and z is as defined in figure 3

Power spectral density of pressure fluctuations

Examples of the power spectral density (PSD) of the pressure fluctuations are plotted in figure 5, for three Reynolds numbers and at fixed $M = 0.9$. The data in figure 5 was measured on the rear face of the cavity and the spectrums have been normalised using the dynamic pressure $Q = 1/2\rho U_\infty^2$ and a time-scale of L/U_∞, where ρ is the static density. For a fixed Mach number, increasing the tunnel stagnation pressure resulted in an associated increase in the Reynolds number ($Re_L = U_\infty L/\nu$) of the

cavity (see figure 1). The values of Re_L are directly proportional to p_0 and hence there is a factor of 3 variation in Re_L, for fixed M. Across this Reynolds number range, there was found to be no effect of Re_L on the fluctuating pressure signals, when normalised with Q. Similar test by [14] and [9] also found that both the non-dimensional fluctuating pressures and the non-dimensional mean pressures did not vary with Reynolds numbers.

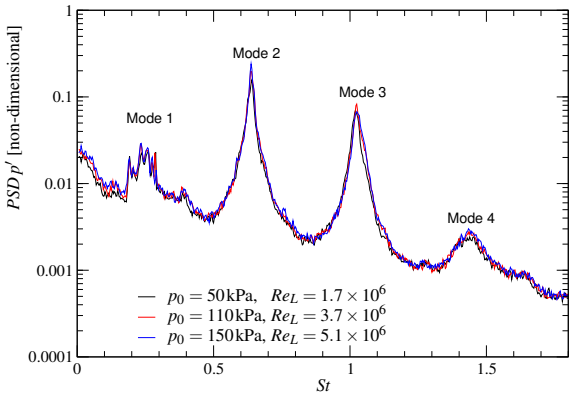

Figure 5: Normalised spectral distribution of pressure on the rear face at $M = 0.9$ for tunnel total pressure conditions of $p_0 =$ 50 , 110 & 150 kPa for $L/D = 5$ case.

Comparisons between the two L/D cases are shown in figure 6, for $M = 1.1$ and for different x/L locations on the cavity base face. The use of inserts to achieve the $L/D = 4$ geometry meant that no sensors were fitted in the rear face for this case. Therefore all comparisons that follow are for base face sensors. The Strouhal number predicted by Rossiter's equation (1) is marked as a gray band corresponding to the empirical range of γ given in [10] for cavity geometries $L/D = 4$ to 5. Differences in the PSDs of the $L/D = 5$ to $L/D = 4$ cases were most evident about mode 4. The $L/D = 5$ data shows two peaks centred about the predicted mode 4, with the higher frequency peak being stronger. Whereas, for the $L/D = 4$, the energy is shifted to the lower frequency peak at mode 4. Further discussions of the mode intensities with Mach number will be given below. However, mode 2 is generally the dominant mode for both L/D ratios.

Resonant frequencies

In general the first 4 Rossiter modes where evident in the pressure PSDs and these peaks are marked on the data of figures 5 and 6. The frequencies of these modes was found using a simple peak detection algorithm that identified the absolute maximum values within a specified frequency band. The algorithm allowed the peaks to be identified in a consistent and automated way. For certain cases facility dependant frequency tones were present in the spectrums, for example due to fan blade passing. Such tones were clearly distinguishable from the Rossiter modes and were rejected from the peak detection algorithm. Figure 7 shows the Strouhal number of the first three Rossiter modes, for both the $L/D = 5$ data and the $L/D = 4$ data. The data is compared to the Rossiter equation (1) using numerical constants $\gamma = 0.248$ for $L/D = 4$ and $\gamma = 0.310$ for $L/D = 5$ with $K = 0.57$ for both cases. The values used for the numerical constants in (1) are based on the empirical values determined in [10]. The data agrees fairly well with the Rossiter equation, with the exception of the $M = 0.3$ data which is generally less than the Rossiter prediction. The difference in Strouhal number modes of the $L/D = 4$ compared to the $L/D = 5$ data appears to be within the experimental scatter and no clear trends can be established.

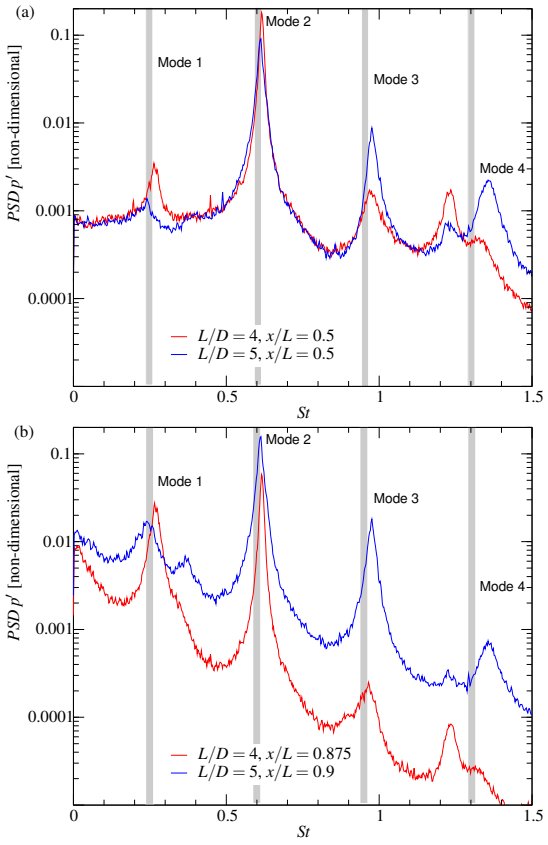

Figure 6: Comparison of normalised PSD of pressure for $x/L =$ 4 and $x/L = 5$ at $M = 1.1$. Data is shown for the base face at locations (a) $x/L = 0.5$ and (b) $x/L = 0.875$ and $x/L = 0.9$.

A modified form of (1) is given in [5] and takes into account the difference between the speed of sound within the cavity and the freestream. For the Mach number range of these experiments the quality of the fit to the data of either (1) or the modified form given by [5] is similar.

Figure 7 confirms the lack of a Reynolds number dependence of the Rossiter tones. For the $L/D = 5$ data the variation in p_0, at fixed Mach, causes a corresponding variation in Re_L. Only the $M = 0.3$ data shows a lack of collapse. However the tones at $M = 0.3$ are relatively weak and less well defined than at the high Mach numbers and this may explain the lack of collapse. As noted above the variation in Re_L (at fixed Mach) did not cause a significant change in the upstream boundary layer thickness (or state, i.e. turbulent versus laminar). Further work is underway to determine the effect of the upstream boundary layer thickness on the cavity tones.

Resonant Intensities

The intensity of the Rossiter frequencies is quantified by measuring the local maximum of the non-dimensional pressure PSD at a given Rossiter mode. Figure 8 shows the non-dimensional mode intensities as a function of Mach number. The results given in it figure 8 were measured on the most aft sensor in the base face of the cavity. It can be seen that mode 2 is the dominant mode and the intensity of this mode increases with increasing Mach number. Modes 1 and 3 show an initial (approximately logarithmic) increase with Mach but at around $M = 0.7$ the intensity of these modes remains either constant or shows a decrease with increasing Mach. For the case of $L/D = 4$ there is a rapid decrease in the intensity of mode 3 with Mach but this behaviour is not seen in the $L/D = 5$ case.

The peak intensities given in figure 8 are in non-dimensional

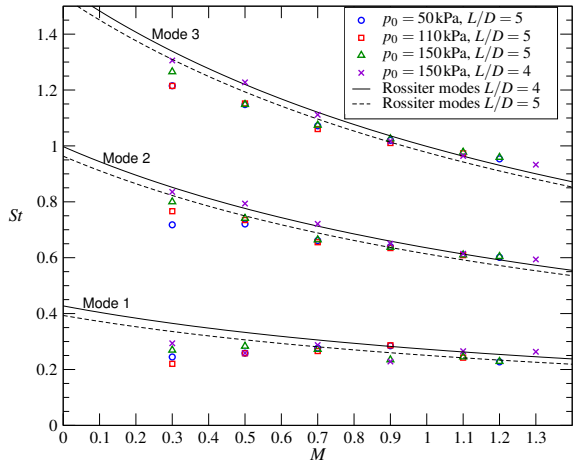

Figure 7: Resonant Strouhal numbers versus Mach numbers.

form, where the scaling factor is $(\rho^2 U_\infty^3 L)/4$ (in units of $\mathrm{Pa}^2/\mathrm{Hz}$). For the mode 2 of the $L/D = 5$ case, there is up to approximately a factor of 100 increase in the non-dimensional energy associated with the peak intensities of mode 2 between $M = 0.3$ and $M = 1.3$. In dimensional form this translates to a factor of 1000 increase in energy.

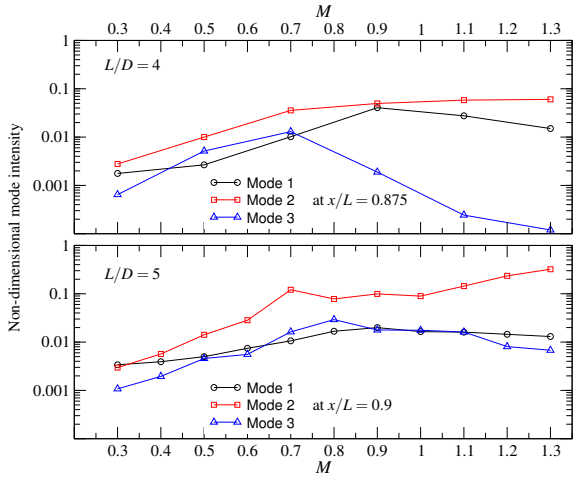

Figure 8: Variation in spectral peak intensity with Mach number, for modes 1 to 3.

Conclusions

The non-dimensional fluctuating pressure signals were found to be insensitive to the cavity Reynolds number for fixed Mach and cavity geometry. This finding is valid for the experimental Reynolds number range of $Re_L = 1.7 \times 10^6$ to $Re_L = 5.1 \times 10^6$. However [14] reached a similar conclusion, based on their experiments of over a much larger Reynolds number range ($Re_L = 1.9 \times 10^6$ to $Re_L = 94 \times 10^6$).

For fixed upstream geometry, a change in the Reynolds number will cause an associated change in the boundary layer at the leading edge of the cavity. So it is possible that sufficiently large changes in Reynolds number may still indirectly effect the nature of the resonance through a change in the upstream boundary layer. Certainly a change from a laminar to turbulent boundary layer is known to effect the resonance [8]. For our experiments, the change in δ/L, associated with a change in Reynolds number, was small and hence it is not possible to draw any conclusions about the effect of this parameter.

The variation in the resonant frequencies with Mach number is consistent with the Rossiter equation (1). The (non-dimensional) intensities of the resonant peaks exhibited a strong Mach number dependency. For $M < 0.7$ there was a logarithmic variation with Mach for modes 1-3, at around $M = 0.7$ the behaviour of the intensities changed and modes 1 and 3 became either flat or decreased with Mach.

When expressed in dimensional form the energy associated with the resonant peaks can increase by 3 orders of magnitude over the Mach number range of the experiments. From a practical point of view, this indicates that the intensities are highly sensitive to flight speed. Mode 2 was found to be the dominant Rossiter mode for all cases studied. Significant difference in the behaviour of mode 3 and higher modes were observed when comparing the $L/D = 5$ to $L/D = 4$ data.

References

[1] Ahuja, K. K. and Mendoza, J., Effects of cavity dimensions, boundary layer, and temperature on cavity noise with emphasis on benchmark data to validate computational aeroacoustic codes, Contractor Report NASA-CR-4653, NASA, 1995.

[2] Block, P. J. W., Noise response of cavities of varying dimensions at subsonic speeds, Tech. Note NASA-TN-D-8351, NASA, 1976.

[3] Clauser, F. H., Turbulent boundary layers in adverse pressure gradients, *J. Aero. Sci.*, **21**, 1954, 91–108.

[4] East, L. F., Aerodynamically induced resonance in rectangular cavities, *Journal of Sound and Vibration*, **3**, 1966, 277–287.

[5] Heller, H. H., Holmes, D. G. and Covert, E. E., Flow-induced pressure oscillations in shallow cavities,, *Journal of Sound and Vibration*, **18**, 1971, 545–546.

[6] Henbest, S. M., Jones, M. B., Watmuff, J. and Blandford, A., Aeroacoustic resonance in a rectangular cavity: Part 2 effect of varying side slip and leading and trailing edge angles, in *18th Australasian Fluid Mechanics Conference*, 2012.

[7] Jones, M. B. and Watmuff, J., Scaling of cavity-flow wind-tunnel data, in *Thirteenth Australian Aeronautical Conference*, 2009.

[8] Karamcheti, K., Acoustic radiation from two-dimensional rectangular cutouts in aerodynamic surfaces, NACA Technical Note NACA-TN-3487, NACA, 1955.

[9] Plentovich, E. B., Chu, J. and Tracy, M. B., Effects of yaw angle and reynolds number on rectangular box cavities at subsonic and transonic speeds, Tech. Rep. NASA-TP-3309, NASA, 1991.

[10] Rossiter, J. E., Wind-tunnel experiments on the flow over rectangular cavities at subsonic and transonic speeds., ARC Reports and Memoranda 3438, Aeronautical Research Council, 1964.

[11] Rowley, C. W., Colonius, T. and Basu, A. J., On self-sustained oscillations in two-dimensional compressible flow over rectangular cavities, *Journal of Fluid Mechanics*, **455**, 2002, 315–346.

[12] Sarohia, V., *Experimental and analytical investigation of oscillations in flows over cavities*, Ph.D. thesis, GALCIT, California Inst. Tech., 1975.

[13] Tam, C. K. W. and Block, P. J. W., On the tones and pressure oscillations induced by flow over rectangular cavities, *Journal of Fluid Mechanics*, **89**, 1978, 373–399.

[14] Tracy, M. B., Plentovich, E. B. and Chu, J., Measurements of fluctuating pressure in a rectangular cavity in transonic flow at high reynolds numbers, Tech. Rep. NASA-TM-4363, NASA, 1992.